Iran. J. Biotechnol. October 2023;21(4): e3445 DOI: 10.30498/ijb.2023.351439.3445

Research Article

Research on Circular RNA Expression Profiles in the Photoaging Mouse Model

Qian Li, Mengbi Lin, Yalin Xie, Jie Zhang, Wei Lai

Department of Dermatology and Venereology, The Third Affiliated Hospital of Sun Yat-sen University, Guangzhou, Guangdong 510630, P.R. China

*Corresponding author: Wei Lai, Department of Dermatology and Venereology, The Third Affiliated Hospital of Sun Yat-sen University, Guangzhou, Guangdong 510630, P.R. China. Tel/ Fax: +86-2085253017, E-mail: laiwei2@mail.sysu.edu.cn

Received: 2023/02/14 ; **Accepted:** 2023/07/12

Background: Nude mouse has been widely used to study photoaging induced by long-term chronic UV exposure. Circular RNAs (circRNAs) have been previously identified in several diseases. However, the roles of circRNAs in photoaging and potential regulatory mechanisms remain unclear.

Objectives: To identify specific circRNAs differentially expressed in photoaged skin and investigate their potential role in aging.

Materials and Methods: In this study, we screened out the microarray data to profile the expression of circRNAs. The circRNAs were analyzed by Gene Ontology (GO) and Kyoto Encyclopedia of Genes and Genomes (KEGG) biological pathway.

Results: 36 circRNAs were identified to be differentially expressed between the UV group and control group (fold change > 1.5; $P < 0.05$), including 6 upregulated and 30 downregulated circRNAs. GO and KEGG biological pathway analyses indicated that the changes in circRNAs were associated with cancer, inflammation, oxidative stress, and metabolism.

Conclusions: This present study revealed a circRNAs expression profiling *in vivo*. These findings not only provide a new possibility to prevent the occurrence of photoaging but also have therapeutic values for photoaging and associated skin diseases.

Keywords: CircularRNA, Mice, Photoaging, Ultraviolet

1. Background

Circular RNAs (circRNAs) are a novel class of non-coding RNA molecules that exhibit a covalently closed cyclic structure, distinct from the linear structure of conventional RNA molecules (1). Over the past decade, circRNA has garnered substantial attention as a potential regulator of gene expression and a mediator of various biological processes (2). CircRNAs have been implicated in multiple diseases, including cardiovascular disease (3), Alzheimer's disease (4), and cancers (5, 6), thereby highlighting their potential as diagnostic and therapeutic targets. Moreover, several studies have indicated that circRNA may play a role in cellular aging (7-9), further adding to the significance of this molecule in the field of molecular biology.

Ultraviolet radiation (UVR) is a form of electromagnetic radiation that is present in both natural (e.g., sun) and artificial (e.g., tanning beds) sources. The UVR can be separated into 3 subtypes: UVA (320-400 nm), UVB (280-320 nm), and UVC (100-280 nm)(10). UVC has the shortest wavelength and is mainly depleted by the ozone layer, so UVA and UVB are significant contributing

factors to photoaging (11). Photoaging, a result of chronic exposure to UVR from the sun, represents a primary form of aging that profoundly impacts human health and well-being. This process is distinguished by several morphological changes in the skin, including wrinkles, rough texture, and hyperpigmentation, which are frequently associated with reductions in denatured collagen and accumulated elastic fibers (11-14). Despite there having been advances in recent years, the molecular mechanisms underlying photoaging still need to be fully understood.

The photoaging nude mouse model is widely used to investigate the physiological and pathological changes induced by ultraviolet. (15-18) Some studies have attempted to explore the molecular changes in ultraviolet-induced *in vitro* models. (19-22) However, due to the vivo experimental limitations, the findings in cellular research are usually difficult to reproduce. (23-25) To better comprehend the molecular mechanisms in photoaging, it is valuable to eliminate unnecessary variables and explore the role of circRNA *in vivo*.

2. Objectives

The objective of this research is to investigate and evaluate the differential expression of circular RNA (circRNA) molecules in photoaged skin tissue in comparison to healthy control skin samples. With microarray analysis, this research provides a valuable overview of the circRNA landscape in photoaged skin. These differentially expressed circRNAs will be subjected to further functional analysis using Gene Ontology (GO) and Kyoto Encyclopedia of Genes and Genomes (KEGG) pathway enrichment analysis. And the biological process (BP), cellular components (CC), and molecular function (MF) of the pathways will allow us to identify those circRNAs and gain insights into the physiological mechanisms underlying photoaging, which could identify possible targets for future therapeutic interventions.

3. Materials and Methods

3.1. Photoaging Model

All experiments were approved by the Medical Ethics Committee of the Third Affiliated Hospital of Sun Yat−sen University (Guangzhou, China). Six 6-week-old female BALB/c nude mice were randomly divided into two groups (n=3 per group) as follows: the UV group (UVA and UVB exposure group) and the control group (naturally aging group). The lab room temperature was 27 ± 1 °C, and the relative humidity was 55 ± 10%. UVA and UVB irradiation occurred in an irradiation device with UVA and UVB tubes (UVP Crosslinker CL-1000, Analytikjena, USA.). The irradiation doses were 10 J/cm^2 and 160 mJ/cm^2 for UVA+UVB, respectively. The distance between BALB/c nude mice and tubes was 10 cm. The frequency of UV exposure was five times a week, and the UVB doses started with 1 minimal erythemal dose (MED; 1 MED = 160 mJ/cm^2) and increased to 4 MED for 8 weeks. (18, 26)

3.2. Histopathological Analysis

After successful modeling, the nude mice were euthanized with CO_2 for 24 hours. Mice dorsal skins were fixed in 4% formaldehyde. We evaluated epidermal thickness and collagen fibers in hematoxylin and eosin (H&E) and Masson's trichrome (MT) by capturing images of the tissues with a light microscope (Leica DM-1000, Germany). We randomly selected three locations from each section to measure, and the data was recorded and calculated via Image-Pro Plus version 6.0 (Media Cybernetics, USA).

3.3. ROS and SOD

Skin ROS and SOD levels (10) were detected using an ELISA kit (Meimian, Jiangsu, China) assays with the manufacturer's recommended protocol.

3.4. Western Blot

The expression of MMP-1 and Collagen1A1 (COL1A1) was verified by Western blot (Gupta *et al*., 2014b). The skin tissues were grounded, then the supernatant was carefully absorbed after centrifugation at 4 °C at 4360.2xg for 30 min. The concentration of protein was evaluated by a BCA kit (Thermo Fisher Scientific, USA). 50μL of protein was separated in 10% SDS-PAGE gel and transferred onto a PVDF membrane. After transfer, the membranes were blocked with 5% skimmed milk powder-TBST. Anti-MMP1 (Proteintech, 10371-2-AP, 1:1000 dilution), Anti-Collagen I (Affinity, AF7001, 1:1000 dilution), and GAPDH (Abcam, ab9485, 1:2500 dilution) as an internal control protein, followed by the secondary antibody was applied to the membrane for 1.5 h at 20 °C. ECL detection was used to expose the protein, and the images were taken at a WSE-6100 LuminoGraph (ATTO, Tokyo, Japan). The amount of target protein

was calculated by gray scanning with ImageJ version 1.50 (National Institutes of Health, USA).

3.5. RNA Extraction and Sample Amplification, Labeling, and Hybridization

The total RNA from skin tissues was extracted using TRIzol® reagent (Invitrogen; Thermo Fisher Scientific, USA) based on the instructions. Detecting the purity of RNA reading the OD by A260/A280 values between 1.8 and 2.0 obtained using a spectrophotometer were considered sufficient (NanoDrop Nd-1000, Thermo Fisher Scientific, USA). After extraction, the RNA was treated to remove linear RNAs and enrich circRNAs, which were transcribed into fluorescently labeled circRNA using the Arraystar Super RNA Labeling Scheme (Arraystar, Inc. USA). The labeled cRNA was hybridized with Arraystar Mouse circRNA Arrays V2.0 (8X15K; Arraystar, Inc.USA) and incubated in an Agilent hybridization oven (Agilent Technologies, Inc. USA) at 65 °C for 17 hours. The hybridized array was managed using an Agilent Scanner G2505C (Agilent Technologies, Inc.USA). The original microarray data were analyzed using Agilent Feature Extraction software version (11.0.1.1; AgilentTechnologies, Inc.)The R software limma (https://bioconductor.org/packages/release/bioc/html/limma.html) was used to set up a range of data analyzing steps, including standardization through high-quality screening. Subsequently, a standard t-test was used to test for differences in these groups. In this study, we selected data with thresholds of >1.5-fold and <-1.5-fold change. A P-value < 0.05 was considered indicative of a statistically significant difference between the 2 groups.

3.6. Bioinformatics Analysis

Gene ontology (GO) was used to performed to indicate the biological process (BP), cellular component (CC), and molecular functions (MF) of all screened-out expressed circRNAs (P< 0.05). Furthermore, the Kyoto Encyclopedia of Genes and Genomes (KEGG) was to reveal the functional categories analysis that determined the involvement of target genes in different biological pathways. Shanghai Kangcheng Biotechnology Co., Ltd completed all the data analysis.

3.7. qRT-PCR

Quantitative reverse transcription polymerase chain reaction(qRT-PCR) was performed from 2 μg total RNA to complementary (c) DNA using the BestarTM qPCR RT kit (2220) (DBI, Inc.Ger.). cDNA amplified supported by directions of the BestarTM qPCR MasterMix (2043) (DBI, Inc.Ger). The experimental instruction was as follows: 95 °C for 2 min, and then 40 cycles at 94 °C for 20 s, 58 °C for the 20s, and 72 °C for 20s. Mouse β-actin was used as a normalization control. GraphPad Prism version 8.00(GraphPad Software Inc. USA) recorded and analyzed the data using a comparative threshold cycle ($2^{-\Delta\Delta Ct}$)method. Sequence pairs are listed in **Table 1**.

3.8. Statistical Analysis

Data analysis was performed using SPSS 25.0 (IBM Corp.USA). All data were presented with the mean ± standard error of the mean. The F-test was used to test the homogeneity of variance. The independent samples student's t-test was used to compare the means between the UV and control groups. P<0.05 was considered to indicate a significant difference.

Table 1. Primer sequences of circRNAs

ID	Sequence (5'- 3')	Product Length(bp)
β-Actin-F	GGGTTGGAAGACCGAGGTTTA	116
β-Actin-R	GCCAGGGTGACAATAATGGACA	
Circ_001194-F	CACGACGAGACACTTACTTACT	153
Circ_001194-R	AGACTGGAATCTTCTTGCTTGA	
Circ_018777-F	TGCTGGCCCTATTGGTCCCC	121
Circ_018777-R	CCTTGGCCCATCCTTTCCTGG	
Circ_33863-F	TGCCAATCACGAAGCTGCCA	147
Circ_33863-R	CAGAGCACAGACGTGCAGGC	

4. Results

4.1. Confirmation of Establishment of UVA+UVB Irradiated Nude Mouse Model of Aging.

4.1.1. Histological Analysis

The histological evaluation was performed to evaluate the effects of UVA+UVB exposure on the skin. **Figure 1** shows a statistically significant increase in epidermal thickness for the UV group (P<0.001). Further analysis using Masson staining revealed alterations in the dermal collagen fibers of the UV group compared to the control group. Specifically, collagen fibers were observed to be curled, twisted, broken, and disorganized.

4.1.2. Detection of Photoaging-Associated Protein and Oxidative Stress-Associated Molecule Expression.

Additionally, **Figure 2** shows that UVA+UVB exposure was found to directly induce the expression of matrix metalloproteinase 1 (MMP-1) (P<0.001) and a corresponding reduction of collagen I (P<0.05). The expression of reactive oxygen species (ROS) and superoxide dismutase (SOD) in the skin of mice in the UV group was observed to be significantly higher compared to the control group (P<0.001).

4.2. CircRNA Expression Profiles in UVA+UVB Irradiated Nude Mouse Model

The analysis of the circRNA expression profiles did

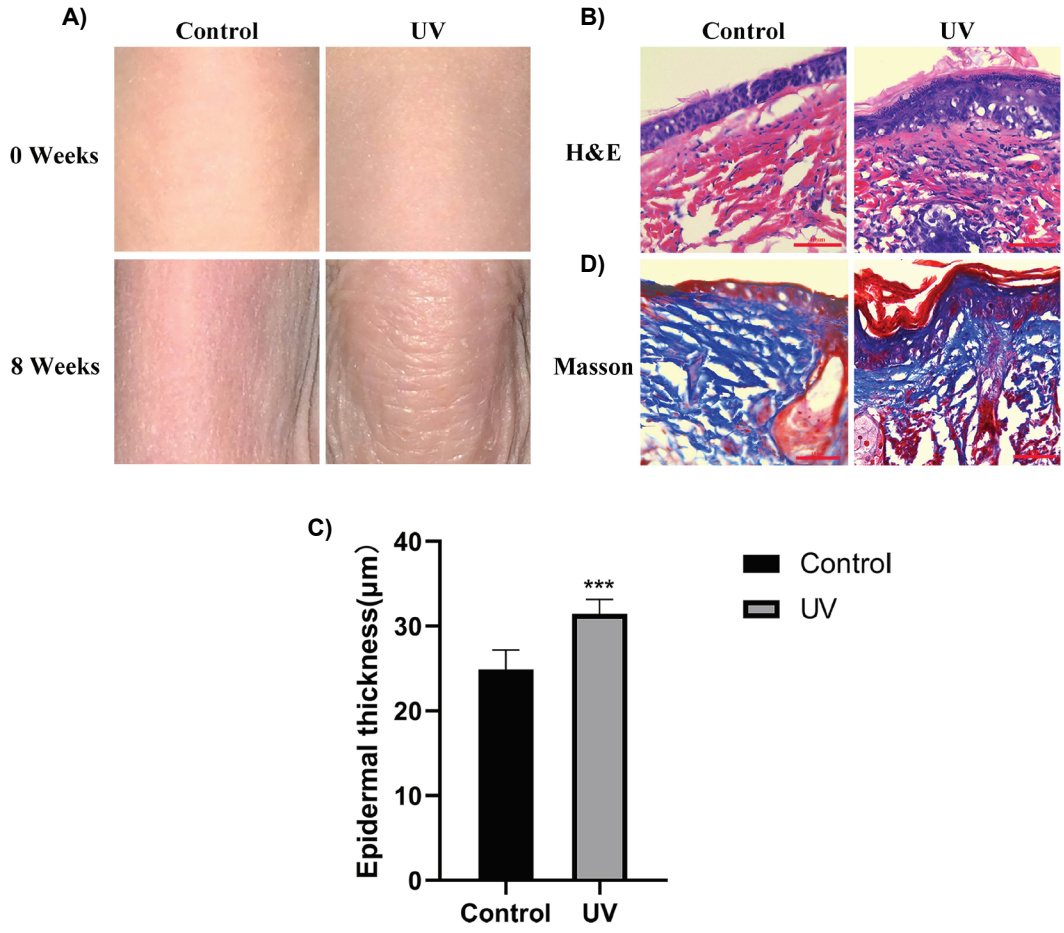

Figure 1. Histological changes between the two groups. A) The view of the dorsal skin of two groups. **B-C)** The HE revealed that the epidermal thickness was significantly increased in the UV group (***P< 0.001). **D)** Masson staining revealed the dermis layer fibers were not well proportioned in the UV group. (400×). HE, Hematoxylin-Eosin; Masson, Masson staining; Control, control group; UV, UVA+UVB group.

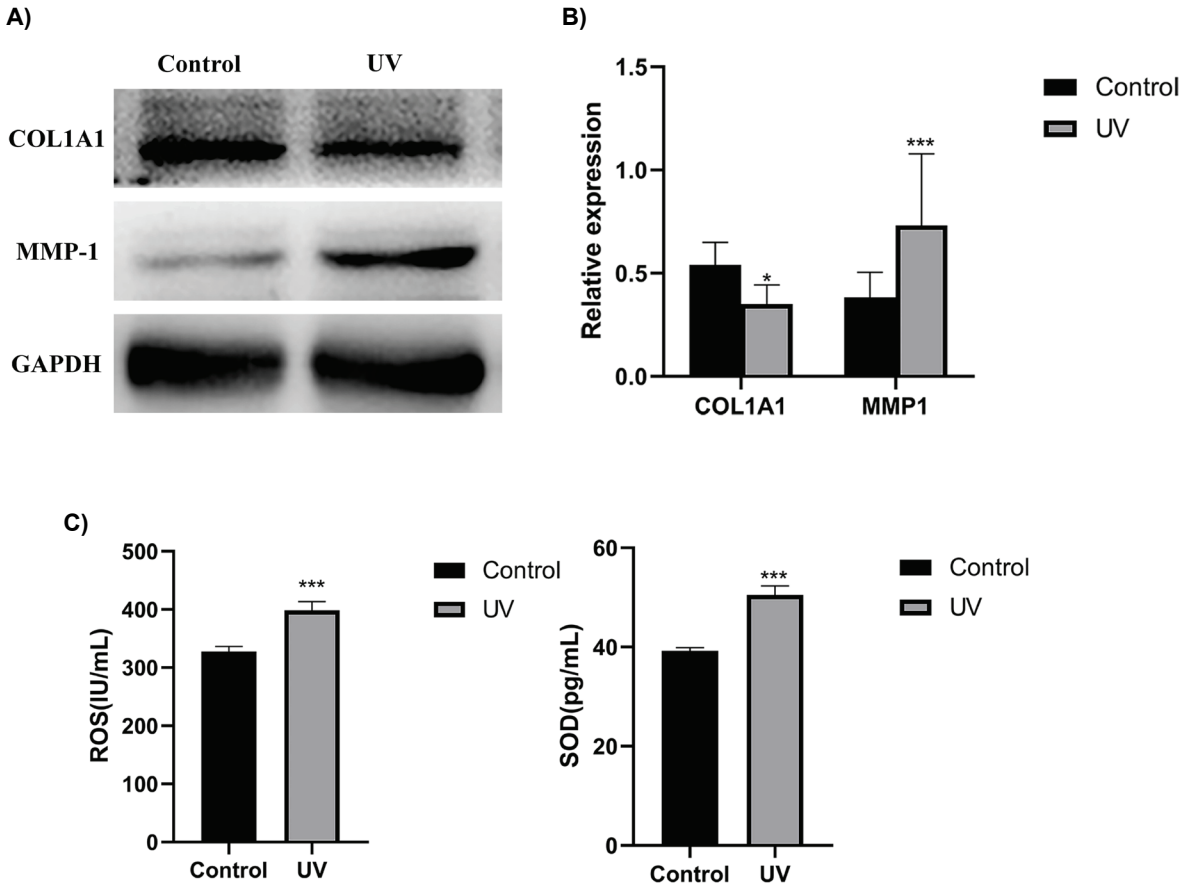

Figure 2. Photoaging model. A-B) Western blot analysis shows that the UV group increased the expression of the collagenases MMP-1 and the degradation of COL1A1(*P< 0.05; ***P< 0.001). **C)** UV triggered the expression of ROS; UV irradiation increased the activity of total SOD in skin tissue. (***p < 0.001).

not reveal any disparities between the group exposed to UVA+UVB radiation and the control group that was not subjected to irradiation (**Fig. 3A**). The identification of screened-out circRNAs between the two groups was performed using Fold Change filtering (**Fig. 3B**), Volcano Plot (**Fig. 3C**), and Hierarchical clustering used to demonstrate the dissimilarity between the UV and the control groups (**Fig. 3D**). The study identified 36 differentially expressed circRNAs (FC>1.5; *P*-value<0.05), consisting of 30 downregulated and 6 upregulated circRNAs (**Table 2**).

4.3. GO and KEGG Enrichments of the Pathways

The results of the bioinformatics analysis revealed the most highly enriched gene functions in the biological process (BP) category to be the cellular process (GO:009987) and cellular metabolic process (GO:0044237). (**Fig. 4A**) The cellular component (CC) category gene functions were found to encompass cellular and anatomical entities and intracellular molecular functions (**Fig. 4B**). The molecular function (MF) category gene functions were identified as binding (GO:0005488), protein binding (GO:00055), and molecular function regulation (GO:0098722). (**Fig. 4C**) The differential expression of circRNAs was primarily associated with pathways related to photoaging, including pathways in cancers, axon guidance, and the MAPK pathway, as well as other pathways such as those involved in the PI3K-Akt pathway, and colorectal cancer. As depicted in **Figure 4D**, the 'MAPK pathway, PI3K-Akt pathway, and TGF-beta pathway had been observed to be associated with photoaging (11, 13, 14).

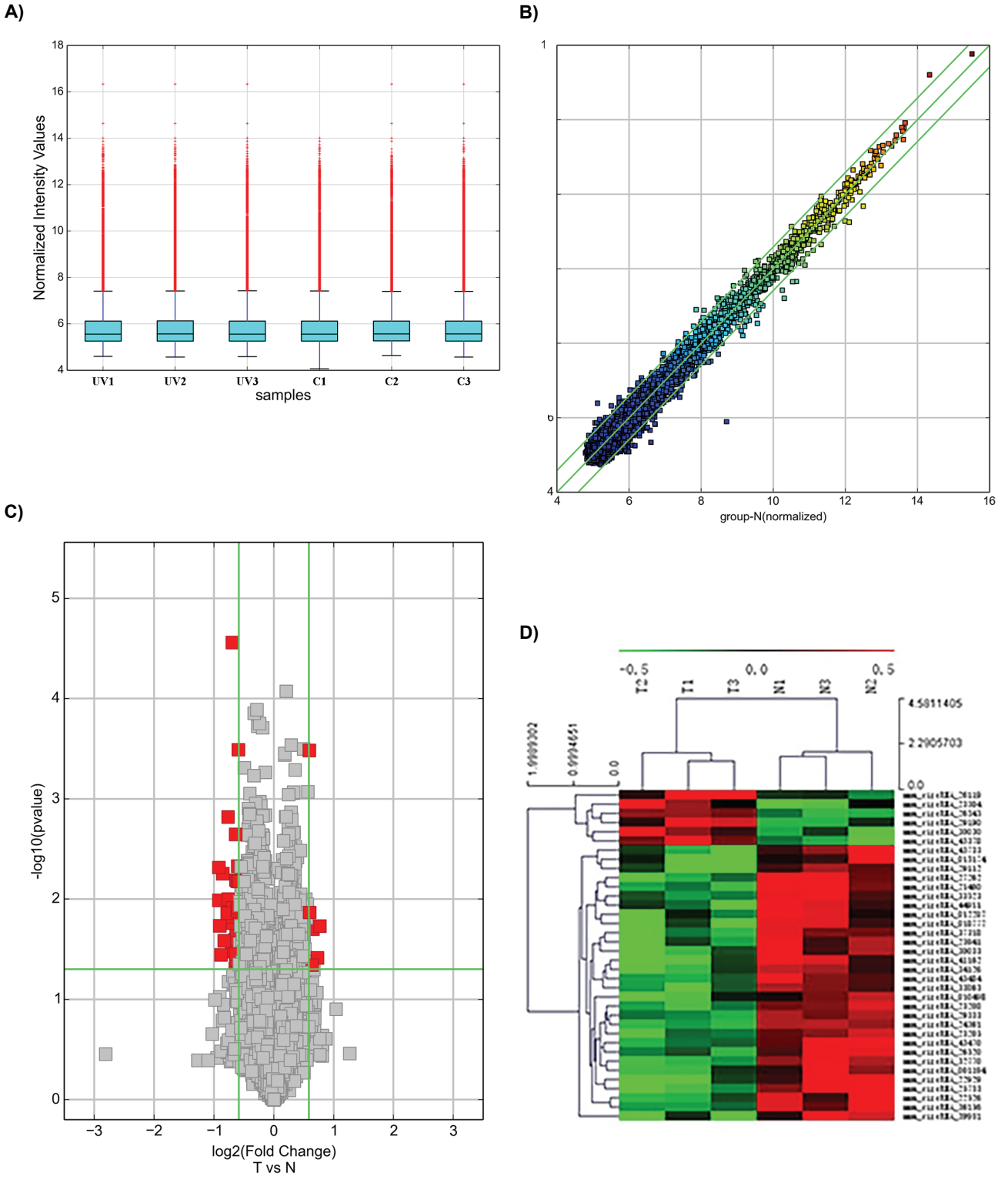

Figure 3. Differentially expressed circRNAs in the UV group and control group. A) The box plot shows the variations in circRNA expression. **B)** The scatter plot and the volcano plot. **C)** Illustrate the distributions of the data in the circRNA profiles (FC>1.5; P<0.05). **D)** The result from hierarchical clustering shows a distinguishable circRNA expression profiling among samples. The heat map shows the differentially expressed circRNAs in samples. Each group consists of three samples. T, UVA+UVB treated group; N, Control group; circRNA, circular RNA; FC, fold change.

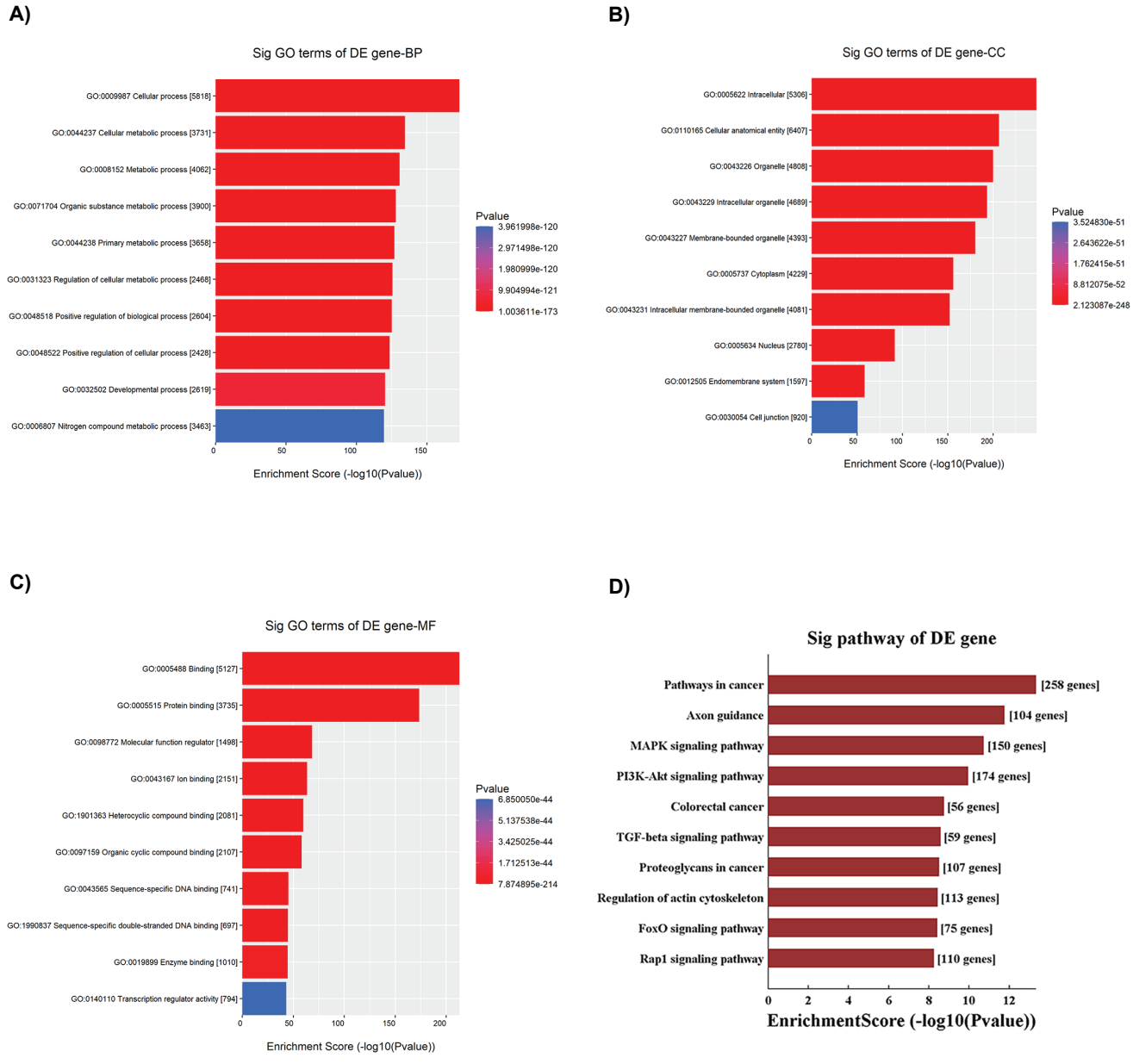

Figure 4. GO and KEGG pathway analysis. GO terms in the categories. A) biological process (BP), **B)** cellular component (CC), and **C)** molecular function (MF). **D)** Top 10 classes of KEGG pathway enrichment terms. GO, Gene Ontology; KEGG, Kyoto Encyclopedia of Genes and Genomes.

4.4. Verification CircRNAs

To corroborate the results of the microarray analysis, qRT-PCR analysis was performed on three randomly selected, significantly differentially expressed circRNAs (circ_001194, circ_018777, and circ_33863). The consequence of it was in accord with the microarray results for circ_001194 and circ_018777. No significant differences were detected for circ_33863 (**Fig. 5**).

Table 2. CircRNAs are differentially expressed following UVA and UVB treatment.

A. Upregulated circRNAs

circRNA	FC(abs)	P-value	regulation	Gene symbol
mmu_circRNA_30030	1.5715	0.0198	up	Paxbp1
mmu_circRNA_26119	1.6550	0.0385	up	Vps41
mmu_circRNA_26545	1.5058	0.0003	up	Exoc3
mmu_circRNA_23304	1.5583	0.0452	up	Phykpl
mmu_circRNA_29190	1.5127	0.0135	up	Usp7
mmu_circRNA_45378	1.7046	0.0184	up	AK170409

B. Downregulated circRNAs

circRNA	FC(abs)	P-value	regulation	Gene symbol
mmu_circRNA_29333	1.5081	0.0003	down	Fgd4
mmu_circRNA_001194 1.5644	0.0252	down	Ubp1	
mmu_circRNA_33863	1.5436	0.0155	down	
mmu_circRNA_36156	1.6808	0.0117	down	Tbck
mmu_circRNA_015174 1.5625	0.0489	down	Rps13	
mmu_circRNA_010498 1.5494	0.0405	down	Dstn	
mmu_circRNA_018777 1.7044	0.0157	down	Col3a1	
mmu_circRNA_45733	1.6315	0.0333	down	Diap2
mmu_circRNA_27262	1.8881	0.0102	down	Arf4
mmu_circRNA_23205	1.5196	0.0047	down	Slit3
mmu_circRNA_43470	1.6963	0.0100	down	Ddx19a
mmu_circRNA_012287 1.5580	0.0351	down	Col1a2	
mmu_circRNA_24361	1.6161	0.0000	down	Prkca
mmu_circRNA_32770	1.7002	0.0015	down	Shoc2
mmu_circRNA_21460	1.8068	0.0056	down	Nvl
mmu_circRNA_22526	1.6198	0.0122	down	AK043505
mmu_circRNA_26520	1.5497	0.0064	down	Zfp65
mmu_circRNA_33523	1.5323	0.0066	down	Epc2
mmu_circRNA_44911	1.5446	0.0206	down	Armc8
mmu_circRNA_25941	1.6128	0.0173	down	Gdi2
mmu_circRNA_41162	1.6833	0.0150	down	Mboat7
mmu_circRNA_37318	1.7162	0.0138	down	Ppap2b
mmu_circRNA_23208	1.5559	0.0023	down	Pank3
mmu_circRNA_30033	1.7745	0.0259	down	Tmem50b
mmu_circRNA_34126	1.5283	0.0131	down	Caprin1
mmu_circRNA_45484	1.5029	0.0067	down	Atp11c
mmu_circRNA_25733	1.8888	0.0048	down	
mmu_circRNA_39951	1.8434	0.0359	down	Calu
mmu_circRNA_22929	1.8726	0.0184	down	Rab1
mmu_circRNA_29112	1.5218	0.0121	down	Pcbp2

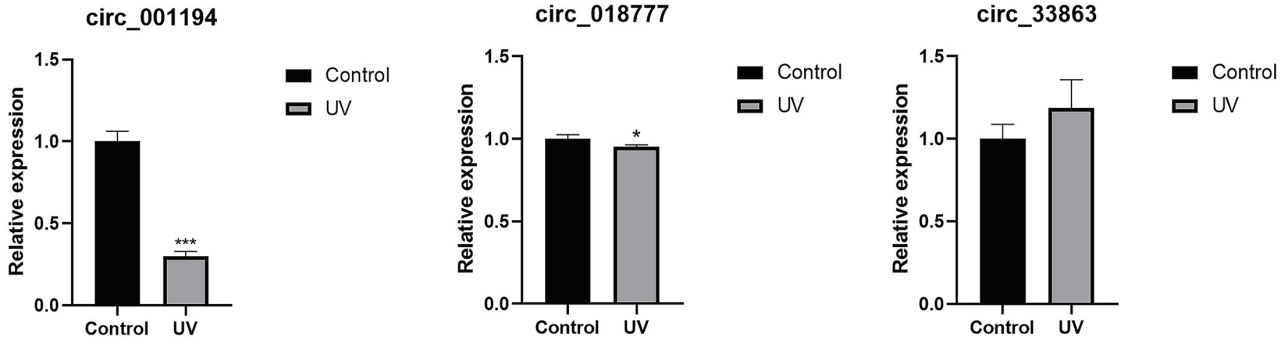

Figure 5. Validation of circRNAs by qRT-PCR. qRT-PCR was performed to validate the expression of circ_001194, circ_018777, and circ_33863 in six skin samples that were continent with the data of microarray chip (* P< 0.05, *** P< 0.001).

5. Discussion

Photoaging, a form of skin aging caused by prolonged exposure to UVR, is a growing concern as UV exposure increases. (12) Due to the complexity of photoaging mechanisms, most studies currently focus on the effect of single-wavelength ultraviolet *in vitro*, such as the exposure to UVA radiation has been demonstrated to result in a substantial enhancement in the discharge of ferrous iron from ferritin in human skin fibroblasts and endothelial cells (27). The administration of resveratrol-enriched rice has been demonstrated to mitigate the adverse effects of UVB-induced oxidative stress on the skin, via the suppression of pro-inflammatory signaling pathways (28). All of the above are not easily replicated *in vivo*. The utilization of photoaging models *in vivo* environment has been shown to provide a more comprehensive understanding of the biological processes associated with skin aging compared to *in vitro* models. In our research, the photoaging mouse model induced by UVA + UVB is a better choice to reproduce the results of photoaging *in vivo* research. Identifying new markers for photoaging will contribute to developing more effective and targeted preventive strategies, ultimately leading to better outcomes for individuals affected by photoaging and light-related diseases.

In past decades, several microRNA-based and lncRNA-based therapeutic interventions have progressed to clinical trials for the treatment of advanced malignancies. These interventions include TargomiR, a microRNA-16 mimic that was used to treat mesothelioma (29); Miravirsen, an anti-microRNA-122 that was used to treat chronic hepatitis C virus infection (30).

Compared with other non-coding RNAs, circRNAs have garnered significant attention recently as a potential treatment for various diseases due to their inherent stability, high abundance, and tissue specificity properties (31, 32). Moreover, alterations in circRNAs expression levels have been linked to several pathological conditions, including cancer, neurodegenerative disorders, and cardiovascular diseases, offering further support for their potential utility as disease biomarkers. (33, 34) Even though circular RNA expression profiles of UVA or UVB have been reported, they both proved the necessity of non-coding RNAs *in vivo* (35, 36).

In this regard, we extracted and screened out 36 differentially expressed circRNAs from the control and UV groups. Out of these, we found 6 upregulated and 30 downregulated circRNAs.

Chen *et al* have revealed that circ_018777 was one of four significantly upregulated circRNAs in acute myocardial infarction (AMI) (37), whose corresponding gene symbol was col3a1. COL3A1 is a gene that encodes type III collagen, which is a major component of the extracellular matrix in the skin. Our previous research revealed that the expression levels of COL3A1 are altered in photoaged skin, and its dysfunction has been reported in the development of skin aging (38). Further research on the relationship between COL3A1 and photoaging would push forward the identification

of new targets for deploying preventive strategies and therapies for skin aging. Identifying these circRNAs further supports the correlation between photoaging and the MAPK pathway (12). These crucial pathways, including ERK, JNK/SAPK, and p38 MAPK, were observed to be associated with photoaging through the regulation of the cell cycle and the synthesis of collagen III (11). Over the past decade, extensive research has established the vital role of circRNAs in regulating various fundamental cellular processes, from protein synthesis to autophagy, and altered circRNAs play a role in the progression of cancer and aging (5).

The principal constraint of this study is the absence of clinical samples set for comparative purposes. Despite these limitations, the data generated from the present investigation furnishes substantial evidence in support of the phenomena of photoaging and light-related pathologies. Furthermore, the prospective circRNAs identified in this study will provide a basis for future extensive studies in this domain.

Acknowledgments

Not applicable.

References

1. Kristensen LS, Andersen MS, Stagsted LVW, Ebbesen KK, Hansen TB, Kjems J. The biogenesis, biology and characterization of circular RNAs. *Nat Rev Genet*. 2019;**20** (11):675-691. doi: 10.1038/s41576-019-0158-7
2. Lu M. Circular RNA: functions, applications and prospects. *ExRNA*. 2020;**2**(1). doi: 10.1186/s41544-019-0046-5
3. Tang Y, Bao J, Hu J, Liu L, Xu DY. Circular RNA in cardiovascular disease: Expression, mechanisms and clinical prospects. *J Cell Mol Med*. 2021;**25**(4):1817-1824. doi: 10.1111/jcmm.16203
4. Dube U, Del-Aguila JL, Li Z, Budde JP, Jiang S, Hsu S, *et al*. An atlas of cortical circular RNA expression in Alzheimer disease brains demonstrates clinical and pathological associations. *Nat Neurosci*. 2019;**22**(11):1903-1912. doi: 10.1038/s41593-019-0501-5
5. Chen L, Shan G. CircRNA in cancer: Fundamental mechanism and clinical potential. *Cancer Lett*. 2021;**505**:49-57. doi: 10.1016/j.canlet.2021.02.004
6. Wu P, Mo Y, Peng M, Tang T, Zhong Y, Deng X, *et al*. Emerging role of tumor-related functional peptides encoded by lncRNA and circRNA. *Mol Cancer*. 2020;**19**(1):22. doi: 10.1186/s12943-020-1147-3
7. Xu K, Chen D, Wang Z, Ma J, Zhou J, Chen N, *et al*. Annotation and functional clustering of circRNA expression in rhesus macaque brain during aging. *Cell Discov*. 2018;**4**:48. doi: 10.1038/s41421-018-0050-1
8. Weigelt CM, Sehgal R, Tain LS, Cheng J, Esser J, Pahl A, *et al*. An Insulin-Sensitive Circular RNA that Regulates Lifespan in *Drosophila*. *Mol Cell*. 2020;**79**(2):268-279 e5. doi:10.1016/j.molcel.2020.06.011
9. Panda AC, Grammatikakis I, Kim KM, De S, Martindale JL, Munk R, *et al*. Identification of senescence-associated circular RNAs (SAC-RNAs) reveals senescence suppressor CircPVT1. *Nucleic Acids Res*. 2017;**45**(7):4021-4035. doi: 10.1093/nar/gkw1201.
10. Pandel R, Poljsak B, Godic A, Dahmane R. Skin photoaging and the role of antioxidants in its prevention. *ISRN Dermatol*. 2013;**2013**:930164. doi: 10.1155/2013/930164
11. Fisher GJ, Kang S, Varani J, Bata-Csorgo Z, Wan Y, Datta S, *et al*. Mechanisms of photoaging and chronological skin aging. *Arch Dermatol*. 2002;**138**(11):1462-1470. doi:10.1001/archderm.138.11.1462
12. Rabe JH, Mamelak AJ, McElgunn PJ, Morison WL, Sauder DN. Photoaging: mechanisms and repair. *J Am Acad Dermatol*. 2006;**55**(1):1-19. doi: 10.1016/j.jaad.2005.05.010
13. Gilchrest BA. Photoaging. *J Invest Dermatol*. 2013;**133** (E1):E2-E6. doi: 10.1038/skinbio.2013.176
14. Weihermann AC, Lorencini M, Brohem CA, de Carvalho CM. Elastin structure and its involvement in skin photoageing. *Int J Cosmet Sci*. 2017;**39**(3):241-247. doi: 10.1111/ics.12372. Epub 2016 Nov 11
15. Hu S, Li Z, Cores J, Huang K, Su T, Dinh PU, *et al*. Needle-Free Injection of Exosomes Derived from Human Dermal Fibroblast Spheroids Ameliorates Skin Photoaging. *ACS Nano*. 2019;**13**(10):11273-11282. doi: 10.1021/acsnano.9b04384
16. Huang J, Tu T, Wang W, Zhou G, Zhang W, Wu X, *et al*. Asiatic Acid Glucosamine Salt Alleviates Ultraviolet B-induced Photoaging of Human Dermal Fibroblasts and Nude Mouse Skin. *Photochem Photobiol*. 2020;**96**(1):124-138. doi: 10.1111/php.13160
17. Hung CF, Chen WY, Aljuffali IA, Shih HC, Fang JY. The risk of hydroquinone and sunscreen over-absorption via photodamaged skin is not greater in senescent skin as compared to young skin: nude mouse as an animal model. Int J Pharm. 2014;471(1-2):135-45. doi: 10.1016/j.ijpharm.2014.05.034
18. Wang YJ, Chang CC, Lu ME, Wu YH, Shen JW, Chiang HM, *et al*. Photoaging and Sequential Function Reversal with Cellular-Resolution Optical Coherence Tomography in a Nude Mice Model. *Int J Mol Sci*. 2022;**23**(13). doi: 10.3390/ijms23137009
19. Tang Z, Tong X, Huang J, Liu L, Wang D, Yang S. Research progress of keratinocyte-programmed cell death in UV-induced Skin photodamage. *Photodermatol Photoimmunol Photomed*. 2021;**37**(5):442-448. doi: 10.1111/phpp.12679
20. Lohakul J, Jeayeng S, Chaiprasongsuk A, Torregrossa R, Wood ME, Saelim M, *et al*. Mitochondria-Targeted Hydrogen Sulfide Delivery Molecules Protect Against UVA-Induced Photoaging in Human Dermal Fibroblasts, and in Mouse Skin *In Vivo*. *Antioxid Redox Signal*. 2022;**36**(16-18):1268-1288. doi: 10.1089/ars.2020.8255
21. Gruber F, Kremslehner C, Eckhart L, Tschachler E. Cell aging and cellular senescence in skin aging - Recent advances in fibroblast and keratinocyte biology. *Exp Gerontol*. 2020;**130**:110780. doi: 10.1016/j.exger.2019.110780
22. Liu W, Yan F, Xu Z, Chen Q, Ren J, Wang Q, *et al.* Urolithin A protects human dermal fibroblasts from UVA-induced photoaging through NRF2 activation and mitophagy. *J Photochem Photobiol B*. 2022;**232**:112462. doi: 10.1016/j.jphotobiol.2022.112462
23. Festing S. On the necessity for animal experimentation.

Bioessays. 2008;**30**(1):94-95. doi: 10.1002/bies.20699
24. Brune K. Animal experimentation in sciences: sadistic nonsense or indispensable necessity? *ALTEX*. 2002;**19**(3):130-136.
25. Robinson NB, Krieger K, Khan FM, Huffman W, Chang M, Naik A*, et al*. The current state of animal models in research: A review. *Int J Surg*. 2019;**72**:9-13. doi:10.1016/j.ijsu.2019.10.015
26. Zhu S, Cai J, Wang J, Feng J, Lu F. Protective Effect of Fat-Tissue-Derived Products against Ultraviolet Irradiation-Induced Photoaging in Mouse Skin. *Plast Reconstr Surg*. 2021;**148**(6):1290-1299. doi: 10.1097/PRS.0000000000008562
27. Smith MJ, Fowler M, Naftalin RJ, Siow RCM. UVA irradiation increases ferrous iron release from human skin fibroblast and endothelial cell ferritin: Consequences for cell senescence and aging. *Free Radic Biol Med*. 2020;**155**:49-57. doi: 10.1016/j.freeradbiomed.2020.04.024
28. Subedi L, Lee TH, Wahedi HM, Baek SH, Kim SY. Resveratrol-Enriched Rice Attenuates UVB-ROS-Induced Skin Aging via Downregulation of Inflammatory Cascades. *Oxid Med Cell Longev*. 2017;**2017**:8379539. doi: 10.1155/2017/8379539
29. Van Zandwijk N, Pavlakis N, Kao SC, Linton A, Boyer MJ, Clarke S, *et al*. Safety and activity of microRNA-loaded minicells in patients with recurrent malignant pleural mesothelioma: a first-in-man, phase 1, open-label, dose-escalation study. *Lancet Oncol*. 2017;**18**(10):1386-1396. doi: 10.1016/S1470-2045(17)30621-6
30. Janssen HL, Reesink HW, Lawitz EJ, Zeuzem S, Rodriguez-Torres M, Patel K, *et al*. Treatment of HCV infection by targeting microRNA. *N Engl J Med*. 2013;**368**(18):1685-1694. doi: 10.1056/NEJMoa1209026
31. Hansen TB, Jensen TI, Clausen BH, Bramsen JB, Finsen B, Damgaard CK, *et al*. Natural RNA circles function as efficient microRNA sponges. *Nature*. 2013;**495**(7441):384-388. doi: 10.1038/nature11993
32. Li Z, Huang C, Bao C, Chen L, Lin M, Wang X, *et al*. Exon-intron circular RNAs regulate transcription in the nucleus. *Nat Struct Mol Biol*. 2015;**22**(3):256-264. doi: 10.1038/nsmb.2959
33. Yang Y, Gao X, Zhang M, Yan S, Sun C, Xiao F, *et al*. Novel Role of FBXW7 Circular RNA in Repressing Glioma Tumorigenesis. *J Natl Cancer Inst*. 2018;**110**(3):304-315. doi: 10.1093/jnci/djx166
34. Zhang M, Zhao K, Xu X, Yang Y, Yan S, Wei P, *et al*. A peptide encoded by circular form of LINC-PINT suppresses oncogenic transcriptional elongation in glioblastoma. *Nat Commun*. 2018;**9**(1):4475. doi: 10.1038/s41467-018-06862-2
35. Lin M, Zheng Y, Li Q, Liu Y, Xu Q, Li Y, *et al*. Circular RNA expression profiles significantly altered in UVA-irradiated human dermal fibroblasts. *Exp Ther Med*. 2020;**20**(6):163. doi: 10.3892/etm.2020.9292
36. Si C, Wang J, Ma W, Hua H, Zhang M, Qian W, *et al*. Circular RNA expression profile in human fibroblast premature senescence after repeated ultraviolet B irradiations revealed by microarray. *J Cell Physiol*. 2019;**234**(10):18156-18168. doi: 10.1002/jcp.28449
37. Wenjiang Chen CC. Microarray analysis of circular RNA expression patterns and circRNA-miRNA-mRNA network in the pathogenesis of acute myocardial infarction. *JACC* J *Am Coll Cardiol*. 2018;**72**.
38. Peng Y, Song X, Zheng Y, Wang X, Lai W. Circular RNA profiling reveals that circCOL3A1-859267 regulate type I collagen expression in photoaged human dermal fibroblasts. *Biochem Biophys Res Commun*. 2017;**486**(2):277-284. doi: 10.1016/j.bbrc.2017.03.028